Published in : Agricultural and Forest Meteorology (2017), v. 247, pp. 21-33
DOI : 10.10i6/j.agrformet.2017.07.008
Status : Postprint (Author's version)

2D PROFILES OF CO_2, CH_4, N_2O AND GAS DIFFUSIVITY IN A WELL AERATED SOIL: MEASUREMENT AND FINITE ELEMENT MODELING

M. Maier[a], B. Longdoz[b,c], T. Laemmel[a], H. Schack-Kirchner[a], F. Lang[a]
[a] *Soil ecology, University of Freiburg, Germany*
[b] *INRA, UMR Ecologie et Ecophysiologie Forestières, UMR1137, Champenowc, F-54280, France*
[c] *TERRA, Gemblowc Agro-Bio-Tech, University of Liège, Gembloux, 5030, Belgium*

KEYWORDS: 2D mapping, Carbon dioxide, Methane, Nitrous oxide, Finite Element Modeling, Gradient method.

ABSTRACT

Soil gas fluxes depend on soil gas concentrations and physical properties of a soil. Taking soil samples for physical analysis into the laboratory strongly modifies soil gas concentrations and also cuts roots that sustain the activity in the rhizosphere. Since microbial processes interact with gas concentrations in soil, we need to study gas transport and production *in situ.*

We developed a method to monitor the transport and production and consumption of carbon dioxide (CO_2), methane (CH_4), and nitrous oxide (N_2O) in soils *in situ* in a two dimensional (2D) profile using tetra-fluoromethane (CF_4) and sulfur hexafluoride (SF_6) as tracer gases and Finite Element Modeling of soil gas transport. Continuous injection of the inert tracer gases and 2D gas sampling in a soil profile allowed for inverse modeling of the 2D profile of soil gas diffusivity. In a second step, the 2D profiles of the production and consumption of CO_2, CH_4, and N_2O were inversely determined.

Soil gas concentrations were monitored in a Scots pine stand in South-West Germany during a rain-free week in the fall. The 2D relative (so as to be independent of gas species) soil gas diffusivity profile showed large horizontal variability. Relative soil gas diffusivity was found to be anisotropic with the vertical direction greater by a factor of 1.26. Topsoil moisture decreased slowly over time resulting in an increase in relative soil gas diffusivity. The soil was found to be a source of CO_2, and a net sink of CH_4 and N_2O, with the highest production (CO_2) and consumption (CH_4, N_2O) occurring in the topsoil. The gas concentration and production profiles of CO_2 were nearly horizontally homogenous, while those for CH_4 showed larger horizontal differences. Net consumption of CH_4 and net production of CO_2 both increased as the soil dried. This occurred despite reverse trends for these variables in the topsoil (0-8 cm depth) which were more than offset by the underlying soil becoming more active. Sensitivity tests showed that the determination of 2D profiles of soil gas diffusivity and production and consumption of CO_2 and CH_4 were more reliable than the estimates for N_2O because the magnitudes of these for N_2O were very low. Our method represents a useful tool for the analyses of soil gas flux heterogeneities and associated microbial processes within soil profiles.

Published in : Agricultural and Forest Meteorology (2017), v. 247, pp. 21-33
DOI : 10.10i6/j.agrformet.2017.07.008
Status : Postprint (Author's version)

1.Introduction

Soils play an important role in the global carbon cycle and in the global balance of the most important greenhouse gases (GHG), carbon dioxide (CO_2), methane (CH_4), and nitrous oxide (N_2O). Chamber methods are widely used and allow for a fast and reliable estimation of soil-atmosphere fluxes of GHG but do not allow for investigating gas production processes within the soil. To understand the dependence of GHG fluxes on environmental factors, it is necessary to understand the spatial dimension of consumption and production of GHG in soils in detail.

Soils are a source of CO_2 from respiration by roots, microorganisms, and macrofauna. Under aerobic conditions soil organic matter is consumed by microbes with emission of CO_2· Under anaerobic conditions emissions can occur as CH_4, which has a much higher greenhouse radiative forcing (Solomon, 2007). CH_4 and N_2O can be simultaneously produced or consumed at various soil micro-sites depending on the availability of oxygen in the local atmosphere (Kuzyakov and Blagodatskaya, 2015; Smith et al., 2003). The balance between overall production and consumption will make a soil a net producer or consumer of CH_4 or N_2O. Thus, understanding soil aeration is central to understanding consumption and production of GHG in soils (Smith et al., 2003).

Soils are complex three dimensional (3D) hierarchical structures consisting of aggregates and pores that result in various physical, chemical and biological properties. On the aggregate scale, large gradients between the center and outer surface of each aggregate of e.g. organic carbon, nutrients, and gas concentrations are usually expected. On the profile scale, vertical gradients of soil color, texture, and nutrient content dominate, and soils are usually assumed to be horizontally homogeneous. Yet, phenomena such as the preferential flow of water through soil shows that the assumption of horizontally homogeneous properties and processes is not always justified. Laboratory studies on soil core samples and soil monoliths have shown that profiles of soil gas concentrations and soil gas diffusivity can vary strongly in the lateral direction (Kühne et al., 2012; Lange et al., 2009), demonstrating the need to include the horizontal component in soil gas studies. The gas environment in laboratory studies is completely different from the natural soil profile which is obvious e.g. for soil samples from anoxic subsoils. Microbial processes in the rhizosphere are different when roots are cut and some processes like methane consumption (von Fischer et al., 2009) can depend on gas concentrations in the soil. Thus, results from laboratory analysis do not represent the natural system and cannot include *e.g.* plant-soil interactions and the spatial interaction between different areas. Therefore, it is necessary to investigate production and transport of soil gases *in situ* and to include spatial patterns.

Assuming molecular diffusion as exclusive gas transport process, *in situ* soil gas fluxes can be calculated based on gas concentration gradients from field measurements and knowledge of the soil gas diffusivity using Ficḱs law (DeJong and Schappert, 1972; Maier and Schack-Kirchner, 2014; Sánchez-Cañete and Kowalski, 2014). Soil gas diffusivity depends on the properties of the diffusing gas and the structure and content of the air filled pores and can be assessed using many semi-empirical diffusivity models available in the literature (Allaire et al., 2008), but which would fit best for a given soil is usually not known (Pingintha et al., 2010). Soil gas diffusivity can be also assessed by analyzing intact soil samples in the laboratory (Jassal et al., 2005; Kühne et al., 2012). Yet, this procedure is destructive and not repeatable, and cannot consider the effect of macro-structures such as stones, coarse roots, or cracks (Lange et al., 2009). Another option is to measure soil gas diffusivity *in situ* (Werner et al., 2004). However, only few such methods are suitable for monitoring soil gas diffusivity over time, and none of these address 2D questions in soil gas transport.

Published in : Agricultural and Forest Meteorology (2017), v. 247, pp. 21-33
DOI : 10.10i6/j.agrformet.2017.07.008
Status : Postprint (Author's version)

Our objectives were to develop a method to monitor, (1), the 2D profile of soil gas diffusivity *in situ* and, (2), the 2D profiles of the production and consumption of CO_2, CH_4, and N_2O in the soil. We developed an automatic system that allows for continuous injection of two tracer gases simultaneously into the soil, and gas sampling at different positions in a soil profile. Inverse modeling of tracer gas transport allows for deriving the 2D profiles of soil gas diffusivity and, in a second step, the 2D profiles of the production and consumption of CH_4 CO_2, and N_2O. To test these methods we conducted a one-week rain-free field campaign and studied how the 2D gas concentration and production profiles changed over time when soil moisture decreased.

2. Materials and methods

2.1 SITE DESCRIPTION AND SOIL CHARACTERISTICS

Measurements were carried out at the experimental forest site Hartheim in the Upper Rhine Valley (South-West Germany, 47° 56' N, 7° 36' E, 201 m above sea level; Maier et al., 2010). The 55-year-old Scots pine stand (*Pinus sylvestris* L.) has dense understory vegetation with grasses and bushes. The mean annual temperature is 10.3°C, the mean annual precipitation is 642 mm.

The soil developed in the former floodplain of the Rhine River on stratified layers of sand and gravel covered by a 0.2-0.6 m thick layer of alluvial loamy silt. The soil is a Haplic Regosol (calcaric, humic) (FAO, 2006) with a pH_{H2O} of 7.8-8.2. Humus type is mull with a 0.02 m litter layer consisting of old pine needles and decomposed leaves. Litter porosity is 75-80% with a moisture content of 5-20%. Intense earthworm activity can be observed. The interface of humus and mineral soil was set to 0 m depth. The texture of the Ah horizon is loamy silt (0-0.2 m depth), followed by a transitional Ah/C horizon with less silt and more gravel (0.2-0.4 m depth), underlain by alluvial sand and gravel. Total porosity φ was 0.77 m^3m^{-3} in 0-0.1 m depth, and 0.64 m^3m^{-3} in 0.2-0.25 m depth (Maier et al., 2012). The organic carbon content is 14.2 kg m^{-2} and concentrates in the Ah and the Ah/C horizons where most of the roots can be found (Goffin et al., 2014; Maier et al., 2010).

2.2 EXPERIMENTAL SET-UP

2.2.1 SOIL GAS SAMPLING

In 2009 two parallel access trenches (0.8 m depth, 1.2 m length, 0.5 m width) were dug with a separation of 2 m. Holes for gas sampling tubes were drilled through the soil between the trenches (Goffin et al., 2014; Goffin et al., 2015; Parent et al., 2013). A 1.5 m long gas-permeable sampling tube (Accurel PPV8/2, Membrana, Wuppertal, Germany) was installed into each of these holes and the trenches were refilled. The nominal depths of the tubes were 0, 0.08, 0.17, 0.35, and 0.68 m, with three replicates of each separated by 0.3 m in the direction along the trenches. Exact positions were documented and included in the gas transport modeling (Fig. 1).

The sampling tubes were connected to the surface via gas impermeable tubes. Each sampling tube was individually accessible using an electromagnetic valve system with 24 channels (Matrix, Ivrea, Italy). When a sampling tube was selected for gas analysis, sampling air circulated in a closed loop through the valve system to the analyzers and back into the respective sampling tube. Tests showed that 20 min were sufficient to equilibrate the air inside the sampling system (analyzers and sampling tubes) with the soil air. Gas concentrations were measured continuously, switching every

Published in : Agricultural and Forest Meteorology (2017), v. 247, pp. 21-33
DOI : 10.10i6/j.agrformet.2017.07.008
Status : Postprint (Author's version)

20 min between the positions, so that every position was measured four times per day. Daily mean values were used for soil gas modeling.

Fig. 1. *2D models of the soil profile. Gas sampling positions and spatial soil compartments are displayed in the conceptual model (zoom section).The interface between litter layer and mineral soil is set to 0 cm depth. The mesh used for Finite Element Modeling consisted of 8032 elements*.

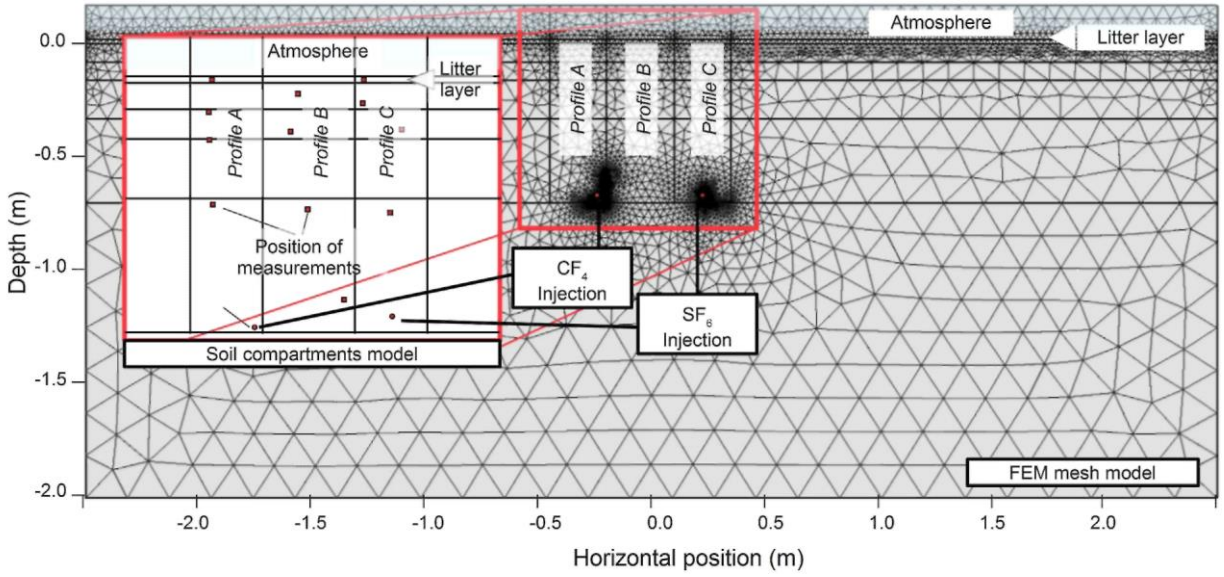

2.2.2 TRACER GAS INJECTION

The two tracer gases (CF_4 and SF_6) were fed separately and simultaneously into the two outer sampling tubes at the 0.68 m depth to measure soil gas diffusivity, as indicated in Fig. 2a and b (middle tube not shown), with CF_4 in the left tube and SF_6 in the right. The tracer gas concentrations at the respective injection positions were not used, since they were affected by the additional diffusive resistance of the sampling tube. The tracer gases can be considered as inert and their solubility in water is low. They were fed in continuously at a constant rate using a peristaltic pump (Ismatec IPN, IDEX Health & Science GmbH, Wertheim, Germany), so that after a certain time a steady state could be assumed for their transport. The injection rates were checked automatically every 6 h by bypassing each gas into a reservoir for 10 min and monitoring the increase in gas concentration (Laemmel et al., 2017). The pump rate was reduced to a minimum (< 0.05 ml min^{-1}) by using pure CF_4 and SF_6. The flow of soil air through the profile induced by the injection was negligible compared to the associated diffusion rates (Laemmel et al., 2017; van Bochove et al., 1998).

Published in : Agricultural and Forest Meteorology (2017), v. 247, pp. 21-33
DOI : 10.10i6/j.agrformet.2017.07.008
Status : Postprint (Author's version)

Fig. 2. *Inversely modeled tracer gas concentrations and D_S/D_0 on Oct 6, 2014. a) Contour plot of the 2D steady-state profile of CF_4. CF_4 was injected at the bottom left, b) Contour plot of the 2D steady-state profile of SF_6. SF_6 was injected at the bottom right, c) The 2D D_S/D_0 profile showed a higher D_S/D_0 in the topsoil < 0.3 m depth and highest values in the litter layer, d) While the topsoil was drying from Oct 1-6, D_S/D_0 in the topsoil increased. Horizontal patterns, i.e. differences between Profile A, B and C persisted.*

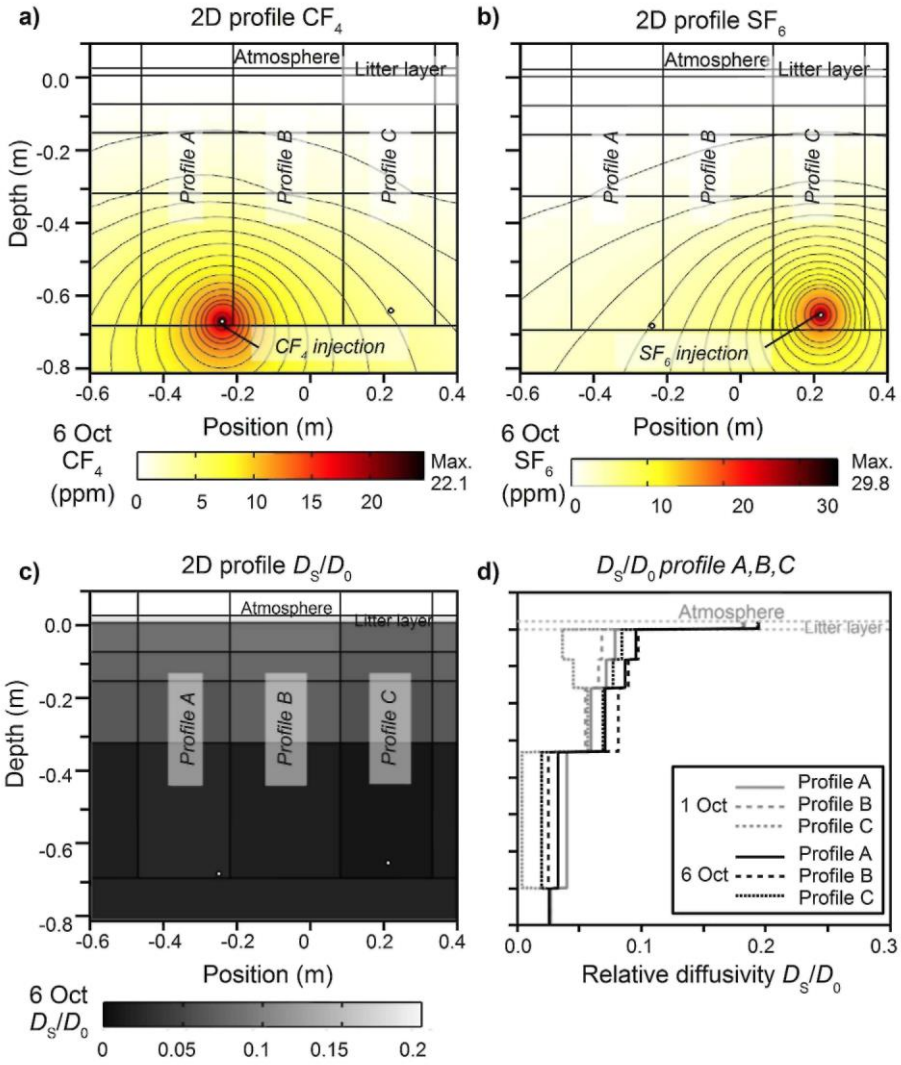

2.2.3 GAS ANALYSIS

The gas concentrations were measured simultaneously in the field for CO_2 and CH_4 using a GreenHouseGas Analyzer Ultraportable (Los Gatos Research Inc., Mountain View, US) and for N_2O, CF_4 and SF_6 using a photoacoustic field gas monitor (Innova 1416, Lumasense, Ballerup, DK). The moisture content of the sampled air was conditioned using a dew point controller set to 8 °C. The stabilization of the water vapor allowed for a high N_2O measurement precision with the photoacoustic gas monitor that was checked against a gas chromatograph in the laboratory prior to the field sampling. Accuracy was 1% of the reading for both field devices and all gases. Precision (standard deviation) was 2 ppb for CH_4 and N_2O, 300 ppb for CO_2, < 1 ppb for CF_4 and SF_6. The time constant of the analyzers was < 1 min. The gas analyzers were stored in an air-conditioned cabinet as the accuracy of both devices would have been affected by temperature changes.

Published in : Agricultural and Forest Meteorology (2017), v. 247, pp. 21-33
DOI : 10.10i6/j.agrformet.2017.07.008
Status : Postprint (Author's version)

2.2.4 CHAMBER MEASUREMENTS

Soil-atmosphere fluxes of all analyzed gases were measured at the last day of the field campaign around noon using a non-steady-state chamber (Maier et al., 2017). Nine steel collars (diameter 15.8 cm, height 17 cm) were installed the day before the measurement. The mobile chamber lid was equipped with a small fan and a vent. Chambers were closed for 15 minutes and air was circulated between the chambers and the gas analysis system described above. Insertion depth of the collars was 2-4 cm and was considered for the calculation of the respective chamber volume. The effective chamber volume was increased by the internal volume of the gas analysis system. Flux calculations were performed using linear regressions versus time of the gas concentration changes of CO_2 and CH_4 (over the first 5 min) and CF_4, SF_6, and N_2O for the full 15 min (Levy et al., 2011). Flux measurements that yielded regressions with P values > 0.05 were set to zero flux.

2.2.5 ANCILLARY MEASUREMENTS

Soil water content was monitored by averaging two horizontally installed probes per depth at 0.07 m and 0.24 m depth (ThetaProbe ML1, Delta-T Devices, Cambridge, UK). Air and soil temperature were routinely monitored using PT100 type sensors. A Vaisala PTB100 pressure sensor was used to measure barometric pressure (Vaisala Oy, Helsinki, Finland). Further meteorological data such as precipitation, relative humidity and wind speed were also measured (Hoist et al., 2008).

Soil physical data were available from earlier studies (Maier et al., 2012). In total more than 60 soil cores of 200 cm^3 volume (height 5 cm) were taken at different sampling depths down to 0.9 m when the gas sampling tubes were installed (Maier et al., 2012). The porosity of the samples was determined by vacuum pycnometry. Soil gas diffusivity was measured for each core using a nonstationary one-chamber method (Maier et al., 2010). Diffusivity measurements were repeated at different soil moisture levels to obtain site and depth specific diffusivity functions (Maier et al., 2012). The soil samples were saturated with water and placed in a filter bed that allowed applying defined water potentials (see Maier et al., 2010).

2.3 GAS TRANSPORT USING FINITE ELEMENT MODELING

2.3.1 BACKGROUND: 1D GAS TRANSPORT MODELING

In a 1D soil profile, the diffusive gas flux (F, mol m^{-2} s^{-1}) can be determined from Ficks law based on gas concentration gradients and soil gas diffusivity using Eq. (1).

$$F = -D_S \rho_a \frac{dC}{dz}$$

where D_S (m^2 s^{-1}) is the effective gas diffusion coefficient of the respective gas species in the soil, ρ_a (mol m^{-3}) is the air molar density, C (mol mol^{-1}) is the gas concentration, and z (m) is the position. D_S depends on the properties of the diffusing gas (diffusivity in free air D_0 m^2 s^{-1}) and the structure of the air filled pores, that is often addressed as tortuosity (Werner et al., 2004). Tortuosity and volume of the air-filled pores depend on the total pore volume and the soil moisture. D_0 is affected by air pressure and temperature (Massman, 1998). Since diffusivity in the gas phase is orders of magnitude largeer than that in the aqueous phase (Wilhelm et al., 1977), diffusion within soil pore water can be neglected in unsaturated soils (Jassal et al., 2004).

Published in : Agricultural and Forest Meteorology (2017), v. 247, pp. 21-33
DOI : 10.10i6/j.agrformet.2017.07.008
Status : Postprint (Author's version)

2.3.2 2D GAS TRANSPORT MODELING USING FINITE ELEMENT MODELING

To facilitate and extend the gradient method we used Finite Element Modeling (FEM) to model soil gas transport and production in 2D using the COMSOL Multiphysics pde solver (Version 5.2 COMSOL Inc., Burlington, Massachusetts, US). Molecular gas diffusion was assumed to be the only transport mechanism in the soil. 2D gas transport in the soil was described using

$$F^i = -D_S^i \rho_a \nabla C^i$$

where D_S^i ($m^2\ s^{-1}$) is the 2D effective soil gas diffusion coefficient tensor of gas species *i* in the soil, in which the horizontal and vertical directions are linked by an anisotropy factor, and C^i (mol mol^{-1}) is the gas concentration of gas species *i*. The relative soil gas diffusivity D_S/D_0, which is independent of gas species, was used to calculate (D_S^i) by multiplying by D_0^i ($cm^2\ s^{-1}$), the D_0 of gas species *i*. D_0^i is 0.21 $cm^2\ s^{-1}$ for CH_4, 0.15 $cm^2\ s^{-1}$ for CO_2, 0.09 $cm^2\ s^{-1}$ for SF_6 (Fuller et al., 1966), 0.14 $cm^2\ s^{-1}$ for N_2O (Marrero and Mason, 1972), and 0.12 $cm^2\ s^{-1}$ for CF_4 (Raw and Raw, 1976) at standard conditions. These D_0^i were modified for changes in barometric pressure and temperature according to Massman (1998).

During the field measurements, soil gas concentrations changed slowly day to day. Test runs with time dependent modeling showed that a steady state was reached within 6-10 h. Since we used daily mean values we assumed steady state diffusion, which simplified the gas budget equations to

$$\rho_a \nabla(-D_S^i \nabla C^i) = P^i$$

where P^i (mol $m^{-3}\ s^{-1}$) represents the production rate density of the gas species *i*. The tracer gases were inert and diffused through the soil matrix without being produced or consumed except for their constant injection at isolated points in the profile (P^i equals a point source). Time dependent modeling would be required in case of fast changes of soil gas concentrations, *e.g.,* after rain, or strong wind events (Maier et al., 2010) or large changes in barometric pressure that can induce advective gas transport in the soil.

2.3.3 TRANSPORT AND PRODUCTION MODELING OF THE FIELD STUDY

The field study gas transport was modeled in 2D in a sufficiently large domain (Fig. 1, width 5 m, depth 2 m). The domain was split into large homogeneous compartments that formed three central profiles (A, *B, C*; see Fig. 1) and side profiles to the left and right. The model included a thin litter layer (0-0.02 m) and an atmospheric layer. The gas sampling locations were more or less in the center of the soil compartments (Fig. 1). The upper boundary of the atmospheric layer was set to the measured atmospheric gas concentrations as Dirichlet boundary condition, and acts therefore as sink and source for the gases. The atmosphere was assumed to be well mixed and the effective diffusivity was set to 10 D_0^i. The sides and the bottom of the modeled domain were impermeable (Neumann boundary condition). The width of the model was stepwise incremented until no effect on the tracer gas distribution in the entire profile was observed, to ensure that the dimension of the modeled area did not affect the modeling outcome within the profiles *A*, *B* and *C*. The tracer gases were injected at 0.68 m (CF_4, left) and 0.64 m (SF_6, right) depth. A physically optimized mesh with 8032 elements was automatically generated by the software and used for the modeling.

Published in : Agricultural and Forest Meteorology (2017), v. 247, pp. 21-33
DOI : 10.10i6/j.agrformet.2017.07.008
Status : Postprint (Author's version)

2.3.4 INVERSE MODELING

2D profiles of D_S/D_0 and P^i were derived by two successive inverse modeling runs, respectively. Each soil compartment in Fig. 1 was assumed to be homogeneous and assigned an independent value for D_S/D_0, P^{CO2}, P^{CH4} and P^{N20}at the beginning. Gas specific production rates (P_i) and D_S/D_0 values were inversely modeled for each of the soil and litter compartments of profile *A*, *B* and *C* down to a depth of -0.7 m. P^i and D_S/D_0 of the wide compartments to the left and right of the central profiles were set to the mean of the respective values of profile *A-C* at the respective depth. Anisotropy of diffusivity (different vertical and horizontal values for D_S) was also used as a fitting parameter since gas transport in soil cannot be considered isotropic (Kühne et al., 2012). The values for the fitting parameters were obtained by inverse modeling such that the objective function minimized the differences between modeled and measured concentrations. For this we used Leven-berg-Marquardt and SNOPT (Sparse Nonlinear Optimizer) algorithms.

To avoid arbitrary results, a special penalty function was used for each fitting parameter, so that the optimization algorithm minimized the sum of the penalty function and the objective function. It consisted of the sum of squares of the difference between neighboring compartments for the variable to be optimized, e.g, the penalty function for P^{CH4}, *(*PF^{CH4}*)* is given by

$$PF^{CH_4} = k_{hor.}^{CH_4}\left(\sum\ (P_{i,j}^{CH4} - P_{i,j+1}^{CH4})^2\right) + k_{ver.}^{CH_4}\left(\sum\ (P_{i,j}^{CH4} - P_{i+1,j}^{CH4})^2\right)$$

where $(P_{i,j}^{CH4} - P_{i,j+1}^{CH4})$represents two horizontally neighboring compartments, and $(P_{i,j}^{CH4} - P_{i+1,j}^{CH4})$ two vertical neighbors. The weight of the penalty function was adjusted individually for the vertical $(k_{ver.}^{CH_4})$and horizontal $(k_{hor.}^{CH_4})$direction and was adapted for each fit parameter *(*D_S/D_0 and P^i*),* to account for the different orders of concentrations and P^i. For P^{CO2} and P^{CH4} the penalization for the horizontal differences was 10 and 2 times stronger than for the vertical direction, respectively, since we expected dominating vertical gradients. For P^{N2O} the same penalization was used for the horizontal and vertical direction. The penalty function for D_S/D_0 was 4 times stronger for the horizontal direction since we expected the vertical variability to be naturally higher. The penalization of differences between litter layer and mineral soil was reduced (by a factor of 0.01) to allow large jumps in D_S/D_0 between these layers. The penalty functions remained unchanged for all days modeled. Daily mean values of the gas concentrations were used. The quality of fit between measured (input) and modeled data was evaluated with the standardized root-mean-square error (SRMSE), normalized by dividing by the minimum to maximum range.

Two consecutive inverse modeling steps were used. First, D_S/D_0 values in all soil compartments and the anisotropy factor were determined using the injection rates and profile measurements of both tracer gases (SF_6, CF_4) simultaneously. Next the P^{CH4}, P^{CO2}, and P^{N2O} values in all soil compartments were determined using the D_S/D_0 compartment values and the CO_2, N_2O, and CH_4 profile measurements.

Fig. 3. *a) Comparison of known ("forward") and inversely modeled D_S/D_0 values. Synthetic tracer gas concentration were modeled forward for two known 2D D_S/D_0 profiles, and then used to inversely model 2D D_S/D_0 profiles again, b) Modeled vs measured SF_6 and CF_4 concentrations showed good agreement and low Standardized Root Mean Square Errors (SRMSE). c) Comparison of inversely FEM modeled D_S/D_0 profiles and D_S/D_0 values derived from diffusivity model (Ma = ; Mo 00 = ; Mo 97 = ; M-Q =). Boxplots are slightly shifted in depth for better visibility. Inversely modeled D_S/D_0 data include 3 lines per profile representing minimum, mean and maximum.*

Published in : Agricultural and Forest Meteorology (2017), v. 247, pp. 21-33
DOI : 10.10i6/j.agrformet.2017.07.008
Status : Postprint (Author's version)

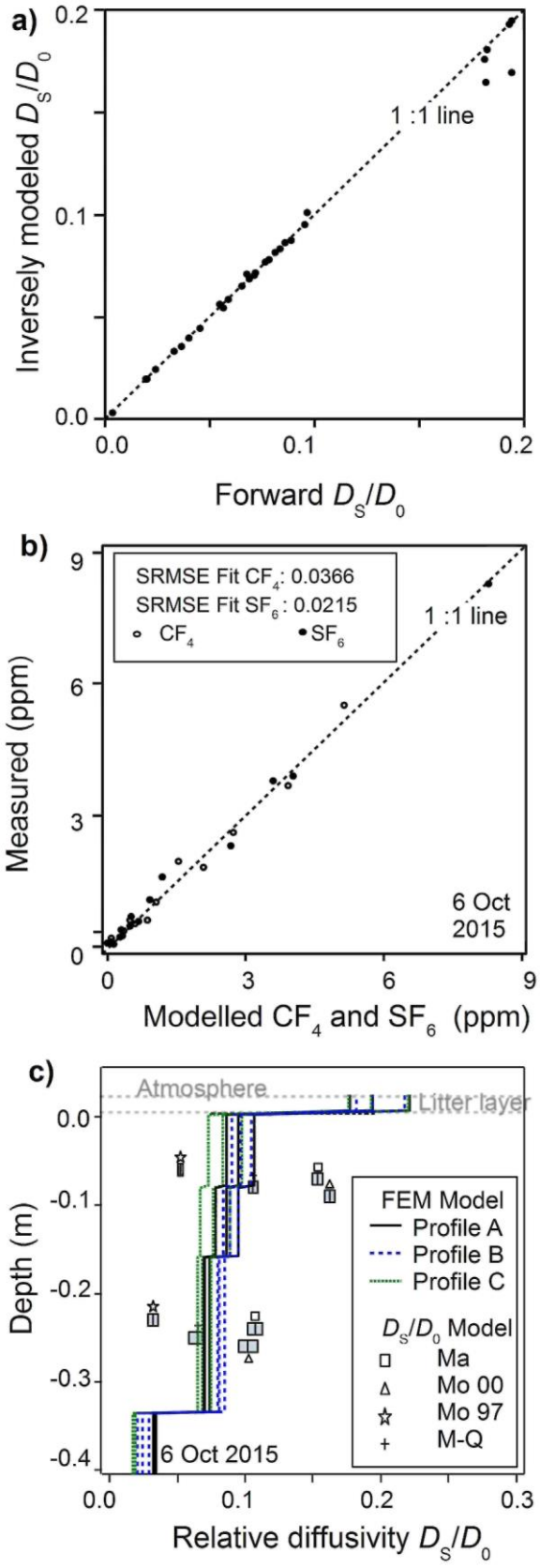

Published in : Agricultural and Forest Meteorology (2017), v. 247, pp. 21-33
DOI : 10.10i6/j.agrformet.2017.07.008
Status : Postprint (Author's version)

***Table 1**. Relative errors (Rel. er)., mean (and standard deviation) between known ("forward") and inversely modeled D_S/D_0 and P^i values per depth of two simulated profiles, (e.g. Rel. er. P^i = P^i (inverse)/P^i(forward)-1).*

Depth (m)	Rel. er. (%)	D_S/D_0	Rel. er. P^{CH4} (%)	Rel. er. P^{CO2} (%)	Rel. er. P^{N2O} (%)
0.01	-4(5)		-9(34)	-2(2)	6(39)
-0.04	1 (3)		1 (2)	0(3)	-2(17)
-0.12	-1 (1)		-4(8)	4(6)	-2(9)
-0.25	0(2)		7(17)	-2(14)	3(15)
-0.6	0(0)		- 26 (68)	4(21)	6(39)

2.3.5 SENSITIVITY AND VALIDATION

To evaluate the sensitivity of the FEM approach we used two approaches: (a) To assess the accuracy and sensitivity of the inverse modeling procedure we synthetically generated data sets of soil gas concentrations at the gas sampling locations with Eqs. (1) and (2) using known 2D profiles of D_S/D_0 and P^i, and then used these concentrations as inputs to the inversion algorithms described above to recalculate D_S/D_0 and P^i, as done for 1D by Novak (2007). Differences between the known input data from the forward model and the inversely modeled 2D profile of D_S/D_0 and P^i were attributed to the inverse modeling procedure. To obtain realistic parameter sets, we used 2D profiles from our model results to generate the synthetic data sets. The evaluations were done in two steps. First the gas concentrations for the synthetic tracer study were simulated. The simulated tracer gas concentrations at the gas sampling locations were used to determine D_S/D_0 of the soil compartments by inverse modeling which were then compared to the known assumed D_S/D_0 values. Next these inverted D_S/D_0 values were used in a forward determination of gas concentrations at the gas sampling locations with known assumed P^{CH4}, P^{CO2}, and P^{N2O} followed by inversion to recalculate the respective P^i in the soil compartments, (b) To consider the sensitivity to measurement errors in the input data we used the daily minimum and maximum soil gas concentrations in addition to the daily mean for the inverse modeling.

To validate the 2D gas transport modeling we compared the modeled soil-atmosphere fluxes with those measured by the field chambers. Modeled 2D profiles of D_S/D_0 were also compared to values derived from well-known soil diffusivity models.

***Table 2**. Standardized root mean square error (SRMSE) between measured and inversely modeled gas concentrations (SF_6, CF_4, CO_2, CH_4, N_2O) on Oct 1 and Oct 6, 2014.*

Date	SRMSE CF_4	SRMSE SF_6	SRMSE CH_4	SRMSE CO_2	SRMSE N_2O
Oct 1, 2014	0.0495	0.0176	0.0141	0.0305	0.0451
Oct 6, 2014	0.0366	0.0215	0.0192	0.0203	0.0409

Published in : Agricultural and Forest Meteorology (2017), v. 247, pp. 21-33
DOI : 10.10i6/j.agrformet.2017.07.008
Status : Postprint (Author's version)

***Table 3**. Comparison of mean values (and standard deviation) of soil-atmosphere fluxes of the tracer gases SF_6 CF_4, and the greenhouse gases CO_2, CH_4, and N_2O based on estimations using chamber measurements and modeled profile fluxes using COMSOL.).*

Method (unit)	Date	CF_4 (nmol m^{-2} s)	SF_6 (nmol m^{-2} s)	CH_4 (nmol m^{-2} s)	CO_2 (µmol m^{-2} s)	N_2O (nmol m^{-2} s)
COMSOL	Oct 1, 2014	0.123 (0.104)	0.073 (0.043)	-1.03 (0.186)	1.68 (0.22)	-0.061 (0.03)
COMSOL	Oct 7, 2014	0.140 (0.106)	0.095 (0.075)	-1.29 (0.049)	1.92 (0.056)	-0.032 (0.010)
Chamber	Oct 7, 2014	0.125 (0.105)	0.109 (0.048	-1.52 (0.195)	3.07 (0.459)	-0.053 (0.080)

***Fig. 4.** Inversely modeled CH_4 concentrations and P^{CH4} a) 2D CH_4 profile on Oct 6, 2014. CH_4 concentrations decreased with soil depth, b) The pattern of the CH_4 Profile A, B and C persisted and shifted to higher CH_4 values from Oct 1 to Oct 6, 2014. c) The 2D P^{CH4} profile showed a high CH_4 consumption in the Ah horizon down to 0.17 m depth, d) Maximum CH_4 uptake shifted from the litter layer on Oct1 to the 0-0.08 m layer on Oct6. The horizontal pattern of P^{CH4} persisted.*

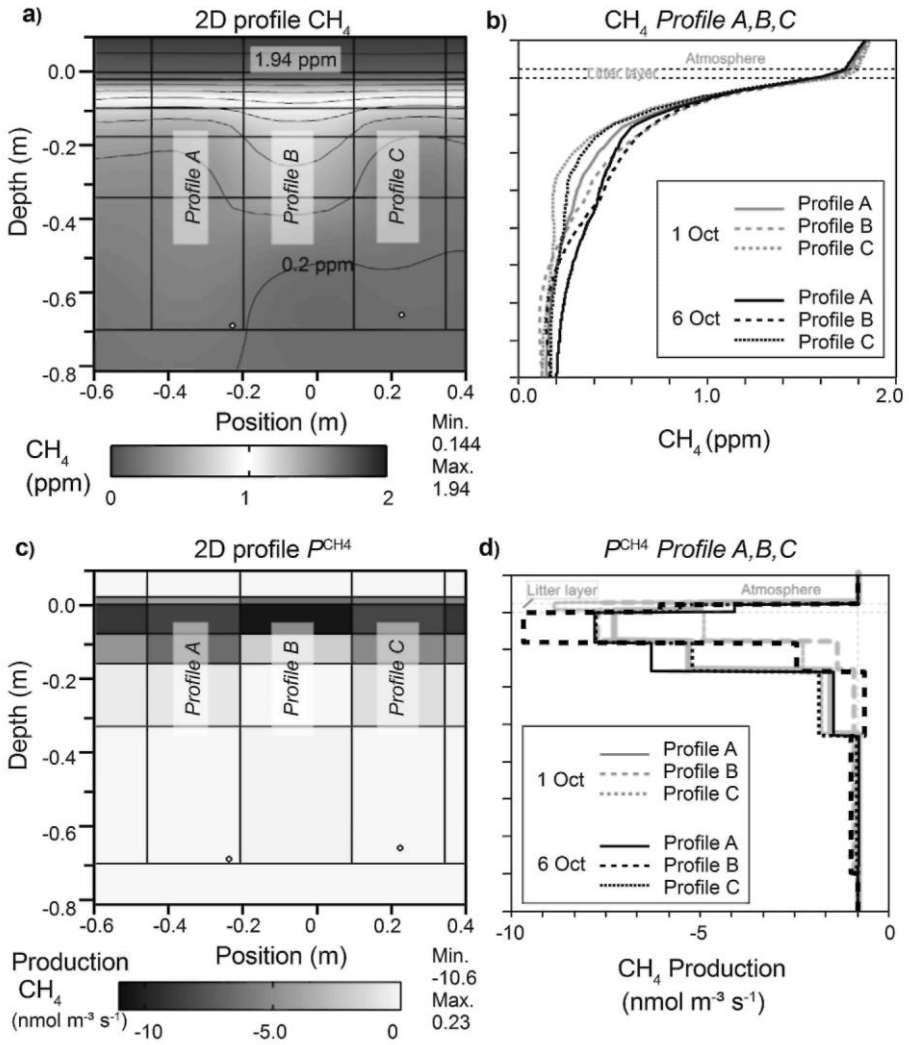

Published in : Agricultural and Forest Meteorology (2017), v. 247, pp. 21-33
DOI : 10.10i6/j.agrformet.2017.07.008
Status : Postprint (Author's version)

2.3.6 REFERENCE VALUES FROM DIFFUSIVITY MODELS

A common way to express the soil gas diffusivity is to use the relative soil gas diffusivity D_S/D_0 that is independent of the diffusing gas.

Reference values of the relative soil gas diffusivity D_S/D_0 were calculated using four well-known diffusivity models from the literature.

1) Ma: $D_S/D_0 = a \cdot \varepsilon^{b}$ with parameters a = 1.50 and b = 2.74 determined at the same site (Maier et al., 2012).
2) Mo 00: $D_S/D_0 = \varepsilon^{2.5} \cdot \phi^{-1}$ (Moldrup et al., 2000).
3) Mo 97: $D_S/D_0 = 0.66 \cdot \varepsilon^{3} \cdot \phi^{-3}$ (Moldrup et al., 1997).
4) M-Q: $D_S/D_0 = \varepsilon^{3.33} \cdot \phi^{-2}$ (Millington and Quirk, 1961).

In these relationships ϕ, (m^3 m) is the porosity and ε (m^3 m^{-3}) is the air-filled pore volume. The air-filled pore-volume was calculated as the difference between porosity and volumetric soil water content. Reference D_S/D_0 values were calculated for both soil moisture measurements at each depth as an indication of variability.

2.4 FIELD MEASUREMENTS

Soil gas concentrations were monitored from Oct 1 to Oct 7, 2014. There was no rain during the field measurements and the mean soil moisture content decreased from 36.3 to 32.8 % in the topsoil (loamy silt) and remained stable at 30 % at 0.24 m depth (loamy sand) (see online supplement). Daily mean air temperature remained stable at 13.0 °C, mean soil temperatures at 0.03, 0.1, 0.2, and 0.4 m depths ranged between 14.0 and 14.5 °C.

SF_6 and CF_4 were continuously injected into the soil at rates of 0.26 µmol s^{-1} and 0.33 µmol s^{-1}, respectively, on Oct 1. The injection rates slowly increased during the measurement period, reaching values of 0.31 µmol s^{-1} and 0.41 µmol s^{-1}, for SF_6 and CF_4, respectively on Oct. 6. Chamber measurements were conducted at the end of the campaign. Reference D_S/D_0 estimates using the formulas above were calculated based on measured soil physical properties and soil moisture contents for Oct. 6.

Published in : Agricultural and Forest Meteorology (2017), v. 247, pp. 21-33
DOI : 10.10i6/j.agrformet.2017.07.008
Status : Postprint (Author's version)

Fig. 5. *a) Comparison of known ("forward") and inversely modeled P^{CH4} values. Synthetic CH_4 concentration were modeled forward for two known 2D P^{CH4} profiles, and then used to inversely model 2D P^{CH4} profiles again, b) Modeled vs measured CH_4 concentrations showed good agreement and low SRMSE. c) Inversely modeled P^{CH4} data (as shown in Fig. 4d) including 3 lines per profile that represent minimum, mean and maximum values.*

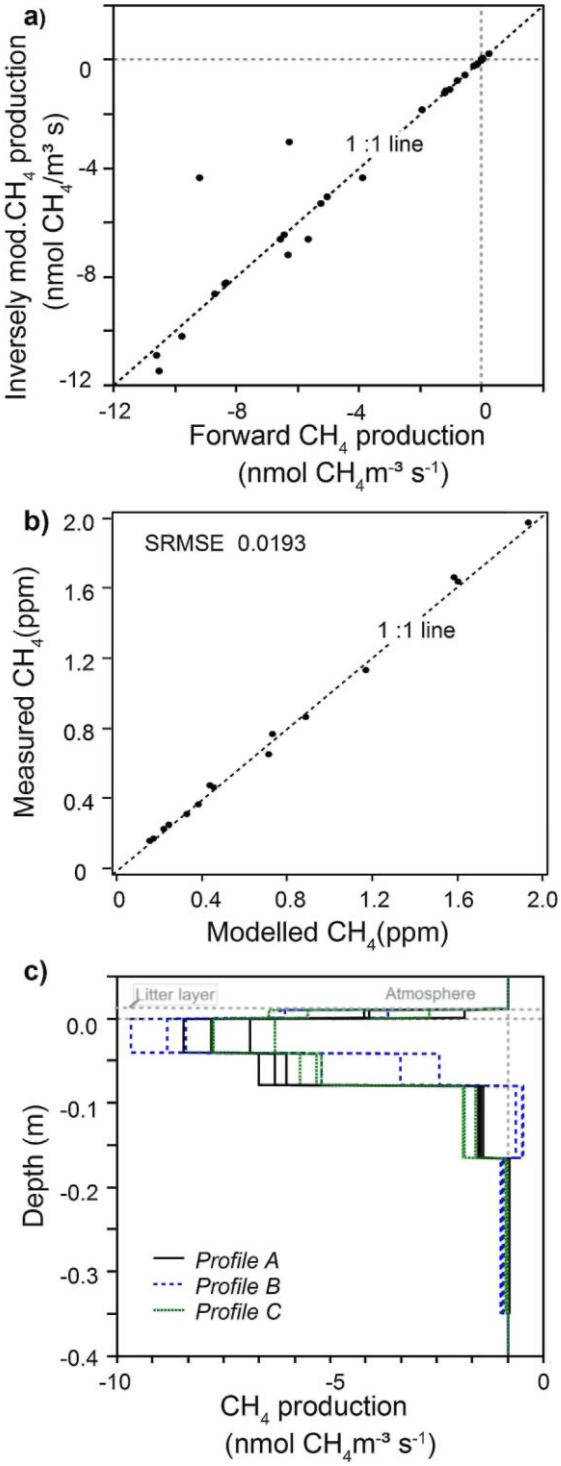

Published in : Agricultural and Forest Meteorology (2017), v. 247, pp. 21-33
DOI : 10.10i6/j.agrformet.2017.07.008
Status : Postprint (Author's version)

3 Results and Discussion

3.1 INVERSE MODELING OF SOIL GAS DIFFUSIVITY

3.1.1 2D PROFILES OF SOIL GAS DIFFUSIVITY

Tracer gas concentrations reached 8.5 ppm SF_6 and 6 ppm CF_4 at the positions next to the respective injection tube (Fig. 2a and b). Maximum concentration of SF_6 was higher than that of CF_4 although the SF_6 injection rate was lower. This was partly due to the lower D_0 of SF_6 compared to CF_4, but also due to the spatial heterogeneity of the gas diffusivity of the soil, as seen from the fact that D_S/D_0 in profile C (SF_6 injection) was lower than D_S/D_0 of profile *A* (CF_4 injection) (Fig. 2c). Tracer gas concentrations increased towards the injection tubes, having concentric isolines (Fig. 2a and b). Tracer gas concentrations decreased slightly during the observation period although the injection rate was slightly increasing (see online supplement). This indicated increasing bulk diffusivity in the soil profile over time that can be explained by the measured decreasing soil moisture content and increasing air-filled porosity.

D_S/D_0 was higher in the topsoil (< 0.3 m depth) than in the deeper soil, with highest values in the litter layer (Fig. 2c and d). The 2D D_S/D_0 profile showed substantial horizontal differences between the topsoil compartments of up to 50%.

Soil moisture in the topsoil decreased faster than in the subsoil during the measurements. Correspondingly, D_S/D_0 of the litter layer and topsoil increased from Oct 1 to Oct 6, while D_S/D_0 changed marginally in the subsoil. The decreasing soil water content in the topsoil resulted in an increasing air-filled porosity and higher D_S/D_0 values.

The clear differences in D_S/D_0 between litter layer, topsoil and subsoil persisted for the whole measurement campaign (Fig. 2d), reflecting the large physical differences of the organic litter layer, the silty topsoil and the sand dominated subsoil. Also the relative spatial pattern persisted with profile C always having the lowest D_S/D_0 (Fig. 2c and d). This indicates that we have to consider relevant spatial patterns of soil aeration that persist over time, with some areas in a soil profile can *e.g.* receive a better supply with atmospheric oxygen or methane, or become anaerobic when soil moisture increases. Studies on soil monoliths showed high spatial heterogeneity in D_S/D_0 as a result of macro-pores like cracks and burrows that can play an important role for soil aeration (Allaire et al., 2008; Lange et al., 2009). Our results showed that we have to expect relevant and persistent 2D patterns in D_S/D_0 even in soils that are considered to be homogeneous as at our study site.

Including an anisotropy factor as a fit parameter in the inverse modeling yielded a better fit for the SF_6 and CF_4 concentrations with a lower SRMSE. The inversely modeled anisotropy factor was 1.26 (vertical D_S/horizontal D_S). This is close to the factor of 1.38 that was observed in a study using soil cores from a forest site and laboratory measurements (Kühne et al., 2012). We argue that both earthworms and gravity are major engineers of this effect. Earthworms preferentially burrow vertical holes while gravity destabilizes preferentially horizontal pores.

Published in : Agricultural and Forest Meteorology (2017), v. 247, pp. 21-33
DOI : 10.10i6/j.agrformet.2017.07.008
Status : Postprint (Author's version)

Fig. *6. Inversely modeled CO_2 and P^{CO2} a) 2D CO_2 profile on 6 Oct, 2014. b) Modeled CO_2 profiles shifted slightly towards lower CO_2 concentrations from Oct 1 to Oct 6. c) The 2D P^{CO2} profile showed the highest CO_2 production in the litter layer and top soil, d) From Oct l to 6, Profile A, B, and C showed a slight decrease in P^{CO2} in the litter layer and increase in the mineral soil.*

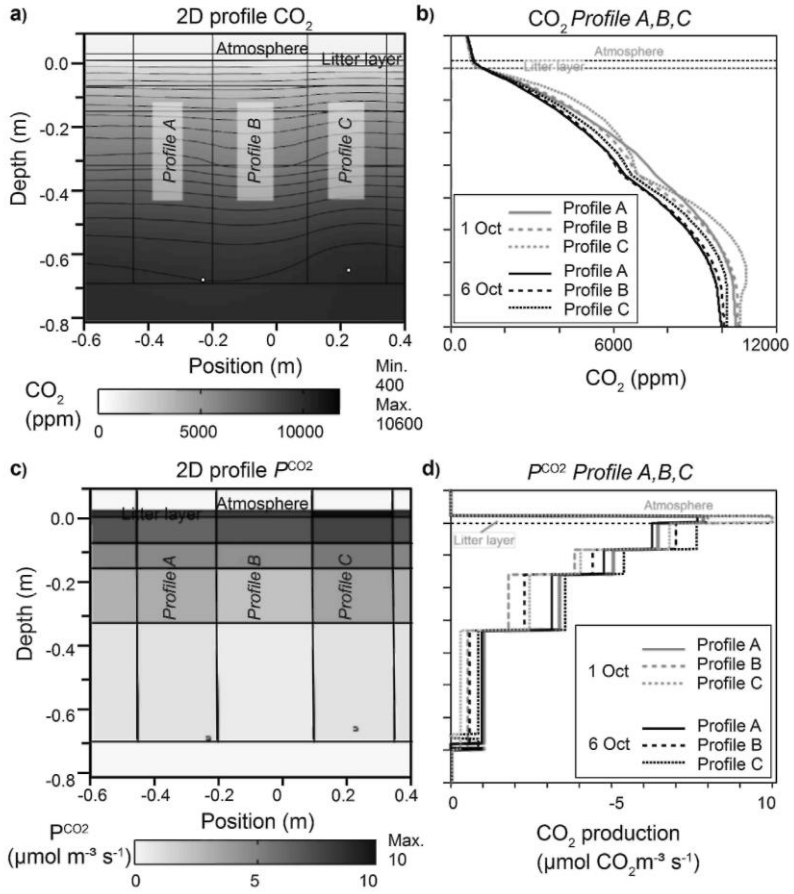

3.1.2 UNCERTAINTY IN THE MODELED DIFFUSIVITY PROFILE AND COMPARISON WITH D_S/D_0 MODELS

The sensitivity test using known ("forward") and inversely modeled 2D diffusivity profiles showed good agreement between the D_S/D_0 values (Fig. 3a). Inversely modeled D_S/D_0 values in the litter layer underestimated known values by at most 4% on average (Table 1). The high D_S/D_0 values deviating from the 1:1 line represent the litter layer in profile *B.* The inverse modeling procedure seemed to best fit D_S/D_0 values at greater depths.

Good agreement between measured and modeled SF_6 and CF_4 concentrations (Fig. 3b) was achieved by inverse modeling of the 2D D_S/D_0 profiles, with standardized root mean square errors SRMSE < 0.05 (Table 2). Including the daily minimum and maximum soil SF_6 and CF_4 concentrations allowed giving a measure of uncertainty in the inversely modeled D_S/D_0 profiles of Oct 6 (Fig. 3c). The range between the replications of the profiles derived from the daily minimum, mean and maximum concentrations were lowest in the subsoil. We think that the FEM approach yielded sensitive estimates of the D_S/D_0 profile. Yet, inaccurately modeled values occurred in the litter layer, where D_S/D_0 values were highest, and concentration gradients were lowest.

SF_6 and CF_4 surface fluxes were estimated using the FEM approach and compared to chamber fluxes. Both methods showed good agreement (Table 3) supporting the concept of the FEM

Published in : Agricultural and Forest Meteorology (2017), v. 247, pp. 21-33
DOI : 10.10i6/j.agrformet.2017.07.008
Status : Postprint (Author's version)

approach. FEM derived D_S/D_0 estimates were compared to values derived from diffusivity models that were calculated for both soil moisture measurements at each depth (Fig. 3c). The D_S/D_0 values derived from diffusivity models and from FEM showed the same decrease with depth. D_S/D_0 derived from the Ma and Mo 00 models are similar, but they changed their order with depth because the Mo 00 model uses an additional parameter. Differences in D_S/D_0 obtained from the different diffusivity models were large. The M-Q and Mo 97 diffusivity models were closest to the FEM derived profiles. Surprisingly, the on-site calibrated Ma model didn't perform as well as the M-Q and Mo 97 models, probably due to plot scale variability in texture and soil structure at this site.

All (SF_6, CF_4, CO_2, CH_4, N_2O) chamber derived fluxes agreed well with the fluxes estimates from the 2D FEM approach (Table 3), which are largely dependent on an accurate D_S/D_0 assessment. Hence, we think that the M-Q and FEM derived D_S/D_0 estimates are most realistic. This also means that estimating the surface flux using the gradient method (Maier and Schack-Kirchner, 2014) yielded better results for the *in situ* determined D_S/D_0 than it would for the Ds/D_0 derived from diffusivity models. The large differences in Ds/D_0 values between the diffusivity models demonstrate the difficulty of choosing the best model *a priori,* and the need to validate a chosen model by measurements on local samples.

Published in : Agricultural and Forest Meteorology (2017), v. 247, pp. 21-33
DOI : 10.10i6/j.agrformet.2017.07.008
Status : Postprint (Author's version)

Fig. 7. *a) Comparison of known ("forward") and inversely modeled p^{co2} values. Synthetic CO_2 concentrations were modeled forward for two known 2D p^{co2} profiles, and then used to inversely model 2D p^{co2} profiles again, b) Modeled vs measured $C0_2$ concentrations showed good agreement and low SRMSE. c) Inversely modeled p^{co2} data (as shown in Fig. 6d) including 3 lines per profile that represent minimum, mean and maximum values.*

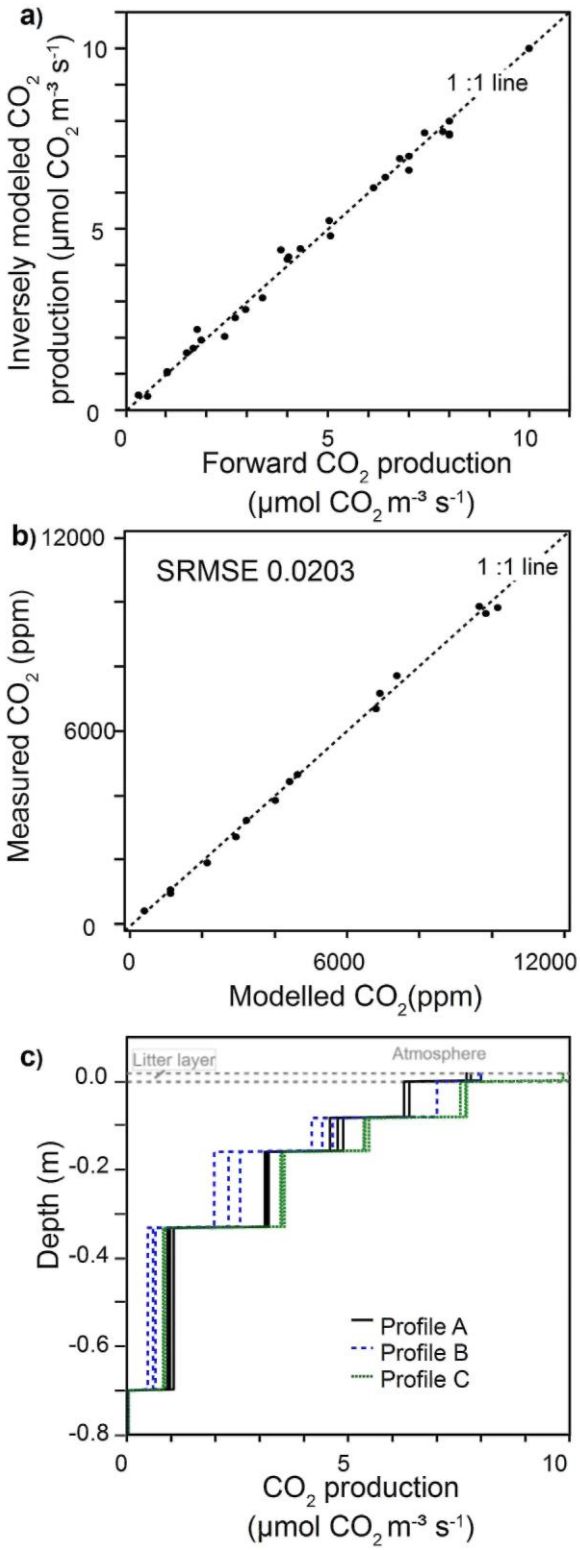

Published in : Agricultural and Forest Meteorology (2017), v. 247, pp. 21-33
DOI : 10.10i6/j.agrformet.2017.07.008
Status : Postprint (Author's version)

3.2 INVERSE MODELING OF PRODUCTION AND CONSUMPTION OF CH_4, CO_2 AND N_2O

3.2.1 CONCENTRATIONS AND CONSUMPTION OF CH_4 IN THE SOIL PROFILE

Chamber measurements and gas transport modeling showed that the soil at Hartheim was a CH_4 sink during the study period (Fig. 4, Table 3), ranging from -1.52 to -1.03 nmol m^{-2} s^{-1}. Soil CH_4 concentrations slowly increased over time, and the spatial pattern between the different sampling positions persisted (see online supplement). Soil CH_4 was always below ambient concentrations and decreased with depth, indicating CH_4 consumption (negative production) throughout the soil profile. Concentrations < 0.2 ppm were reached at depth > 0.5 m (Fig. 4a). CH_4 concentrations between 0.15 and 0.4 m depth were higher in profile *B* than in the other profiles (Fig. 4b).

FEM showed that more than 85% of the CH_4 consumption occurred in the top 0.2 m of the soil where the atmospheric CH_4 supply was the best, reaching -10.6 nmolm^{-3} s^{-1} (Fig 4c and d). The layers below received less CH_4 and CH_4 consumption rates were lower. A similar decrease in CH_4 consumption with depth was observed in all profiles, yet horizontal differences between the profiles were substantial (Fig. 4c and d). Profile *B* showed the highest CH_4 consumption in the topsoil, while the CH_4 consumption in the subsoil was the lowest (Fig. 4d). The observed low CH_4 consumption does not necessarily mean that the microbial composition in this compartment was different; it could also result from the reduced supply due to CH_4 consumption in the soil above.

CH_4 concentrations increased slowly at all measurements locations over time, *e.g.* at 0.17 m depth from 0.40 to 0.49 ppm (see online supplement). Inverse modeling of P^{CH4} showed that the higher CH_4 concentrations resulted from the higher diffusivity and - counter-intuitively - a higher CH_4 consumption. The higher diffusivity led to a better supply with CH_4 stimulating a higher methanotrophic activity, so that deeper layers became more active. Maximum methanotrophic activity shifted from the litter layer (Oct 1) down into the topsoil (Oct 6) over time (Fig. 4d), probably because the litter layer (including mineral compounds) became too dry. Other studies (Adamsen and King, 1993; Karbin et al., 2016; Niklaus et al., 2016; Rosenkranz et al., 2006;) also showed that CH_4 consumption is highest in the top centimeters of the mineral soil and that a decreasing soil water content is often associated with a higher CH_4 consumption (Borken and Beese, 2006; Butterbach-Bahl et al., 2002; Hartmann et al., 2011). Stiehl-Braun et al. (2011) observed that the most active zone of CH_4 consumption shifted downward within the soil profile during a drought. Although we were far from experiencing a drought, a similar shift of CH_4 consumption was observed. This could be explained by a better supply of atmospheric CH_4 to deeper layers due to increasing soil gas diffusivity. Our observation supports the hypothesis that diffusion of atmospheric CH_4 into the soil is the main limiting factor for CH_4 oxidation in upland forest soils (Ball et al., 1997; Smith et al., 2003).

CH_4 can be consumed and produced at the same time within a soil profile (Butterbach-Bahl et al., 2002) and this possibly occurred in our soil. It is important to note that all P^{CH4} rates are net rates and that this can always include CH_4 production, *e.g.* in oxygen depleted zones within aggregates (Kuzyakov and Blagodatskaya, 2015). Approaches using the isotopic signatures of CH_4 can help answer questions of the partitioning between sink and source (Fischer and von Hedin, 2002), and would further improve the spatial mapping of methanotrophic and methanogenic activity in the soil.

Published in : Agricultural and Forest Meteorology (2017), v. 247, pp. 21-33
DOI : 10.10i6/j.agrformet.2017.07.008
Status : Postprint (Author's version)

3.2.2 UNCERTAINTY IN THE MODELED CH_4 CONSUMPTION PROFILE

A sensitivity test using known ("forward") and inversely modeled 2D P^{CH4} profiles showed generally good agreement between the P^{CH4} values (Fig. 5a). Yet, inverse modeling underestimated mean P^{CH4} in the litter layer by 9% (Table 1) resulting from a substantial underestimation in the litter layer in the profile *B* (2 points left of the 1:1 line in Fig. 5.a). The relative error was also large in the subsoil, as a result of P^{CH4} values close to zero; absolute P^{CH4} errors were small in this case.

Good agreement between measured and modeled CH_4 concentrations (Fig. 5b) was achieved by inverse modeling of the CH_4 profiles, with SRMSE < 0.02 (Table 2). Chamber measurements and FEM derived soil-atmosphere CH_4 fluxes showed good agreement on Oct 7 (Table 3). Including daily minimum and maximum soil CH_4 concentrations in the inverse modeling on Oct 6 confirmed the vertical pattern in the P^{CH4} and the horizontal differences between profiles *A-C* (Fig. 5c). The Min-Max P^{CH4} values showed a wider range in profile *B* in the upper soil, this can be interpreted as a higher uncertainty.

Fig. 8. *Inversely modeled N_2O and P^{N2O} profiles, a) 2D profile of N_2O concentrations on Oct 6. b) N_2O concentration profiles had a minimum around 0.3 m depth. The atmospheric N_2O concentration increased slightly by 0.015 ppm from Oct 1-6 and the whole gas profile was shifted from Oct 1 to 6. c) On Oct 6, the topsoil was taking up N_2O and the subsoil tended to N_2O production on Oct 6. d) The pronounced N_2O uptake in 0.07-0.15 m depth on Oct 1 leveled out by Oct 6.The 2D P^{N2O} profile changed substantially by Oct 6 and the pronounced uptake in the topsoil leveled out.*

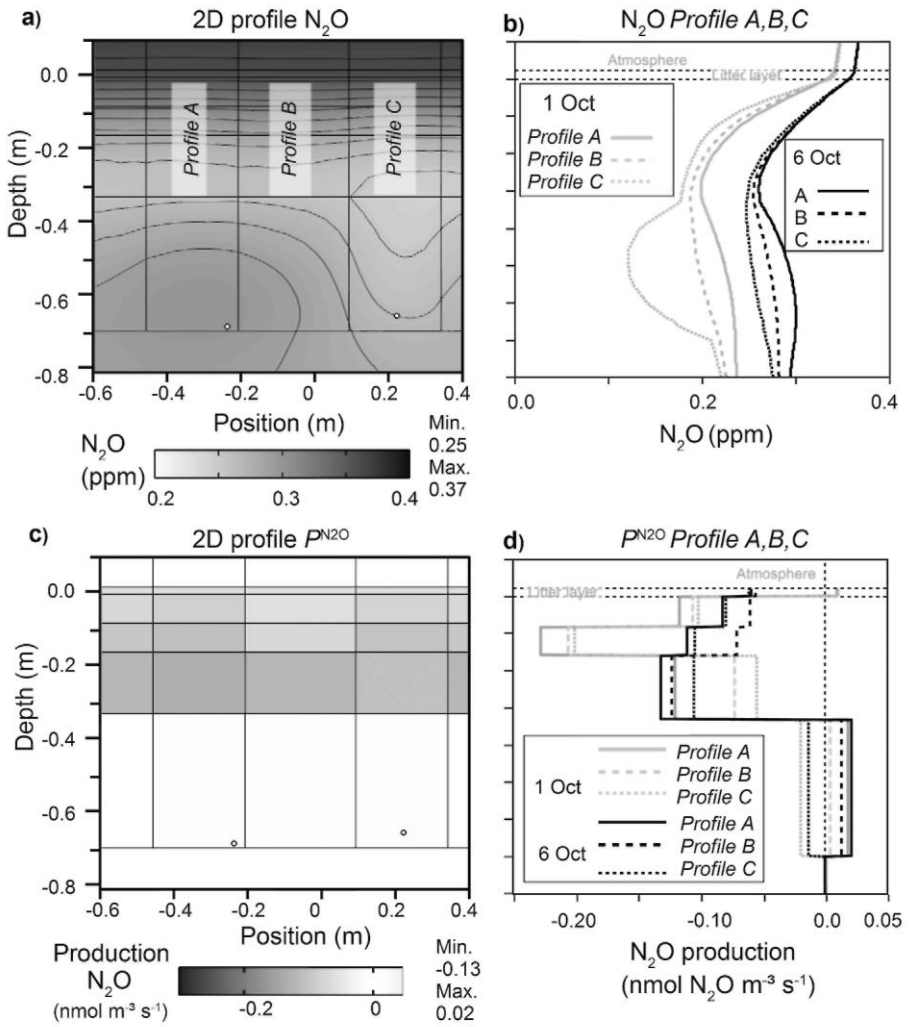

Published in : Agricultural and Forest Meteorology (2017), v. 247, pp. 21-33
DOI : 10.10i6/j.agrformet.2017.07.008
Status : Postprint (Author's version)

3.2.3 CONCENTRATIONS AND PRODUCTION OF CO_2 IN THE SOI PROFILE

Measurements and modeling showed that the soil-atmosphere flux of CO_2 at Hartheim represented the largest GHG flux during our study (Table 3), ranging from 1.68 to 3.07 µmol m^{-2} s^{-1}. Soil CO_2 concentrations slightly decreased with time (see online supplement). CO_2 concentrations increased with depth, reaching > 10000 ppm (Fig 6a and b). Most of the CO_2 was produced in the top 0.3 m (Fig. 6c and d), which is also the most intensively rooted zone (Goffin et al., 2014). P^{CO2} reached 10 µmol m^{-3} s^{-1} in the litter layer (Fig. 6c and d). The subsoil > 0.35 m depth also contributed to the CO_2 production. The modeled P^{CO2} profiles agreed well with that found by Goffin et al. (2014) at the same site and other sites where most of the soil CO_2 originates from the upper soil layers (Davidson et al., 2006; Novak, 2007).

Horizontal differences in CO_2 and P^{CO2} were observed (Fig. 6), but they were less pronounced than differences in D_S/D_0 or P^{CH4}. We conclude that soil respiration is not affected by soil gas diffusivity as long as the soil is well aerated, but that soil respiration rather depends on the homogenous distribution of roots and organic carbon at this site.

Soil CO_2 efflux (= sum of P^{CO2} per area) increased during the monitoring period by 14% (Fig. 6d, Table 3), despite the fact that soil CO_2 concentrations slightly decreased (from 10500 ppm to 9800 ppm at 0.65 m depth, see online supplement). This might seem counterintuitive at the first glance, but can be easily explained by the increase in D_s/D_0 (Fig 2d). The increase in total soil respiration from Oct 1 to Oct 6 was due to the increase of P^{CO2} in the mineral soil while P^{CO2} in the litter layer decreased. This decrease probably resulted from litter drying and becoming biologically less active, as it was also observed for P^{CH4}

3.2.4 UNCERTAINTY IN THE MODELED CO_2 PRODUCTION PROFILE

Known ("forward") and inversely modeled 2D P^{CO2} profiles showed good agreement (Fig. 7a). While the mean P^{CO2} values agreed well in all depths (Table 1), the standard deviation increased with depth, indicating that the horizontal variability was not correctly reflected. Since P^{CO2} values were small in the subsoil, absolute P^{CO2} errors were still small.

Good agreement between measured and modeled CO_2 concentrations (Fig 7b) was achieved by inverse modeling of the CO_2 and P^{CO2} profiles, with SRMSE < 0.04 (Table 2). Including daily minimum and maximum soil CO_2 concentrations Oct 6 yielded narrow minimum-maximum ranges for P^{CO2} iΠ profile *A&C,* and slightly larger uncertainty ranges for profile *B* (Fig 7c). These uncertainty ranges were small compared to the changes in the 2D P^{CO2} profiles between Oct 1-6. The FEM derived CO_2 flux was 37% lower than the FEM derived flux (Table 3). This can be attributed to CO_2 produced in the litter layer that hardly affects the CO_2 concentrations. As a result, the uncertainty of P^{CO2} estimation in the litter layer was higher and lead to a deviation between gradient based flux estimations and chamber measurements (Davidson and Trumbore, 1995; Maier and Schack-Kirchner, 2014). Studies comparing chamber method and gradient flux method yielded better agreement when the soil surface was dry and inactive (Myklebust et al., 2008; Tang et al., 2003; Tang et al., 2005; Vargas and Allen, 2008). The litter layer was still moist in our study. Davidson and Trumbore (1995) used the flux difference between gradient flux method and chamber measurements to derive the litter borne soil respiration, in our case this would be 37% of the chamber measured efflux. This means, that the P^{CO2} in the litter layer was probably much higher than estimated by the FEM.

Published in : Agricultural and Forest Meteorology (2017), v. 247, pp. 21-33
DOI : 10.10i6/j.agrformet.2017.07.008
Status : Postprint (Author's version)

Fig. 9. *a) Comparison of known ("forward") and inversely modeled P^{N2O} values. Synthetic N_2O concentration were modeled forward for two known 2D P^{N2O} profiles, and then used to inversely model 2D P^{N2O} profiles again, b) Modeled vs measured N_2O concentrations showed good agreement and low SRMSE. c) Inversely modeled P^{N2O} data (as shown in Fig. 6d) including 3 lines per profile representing minimum, mean and maximum values.*

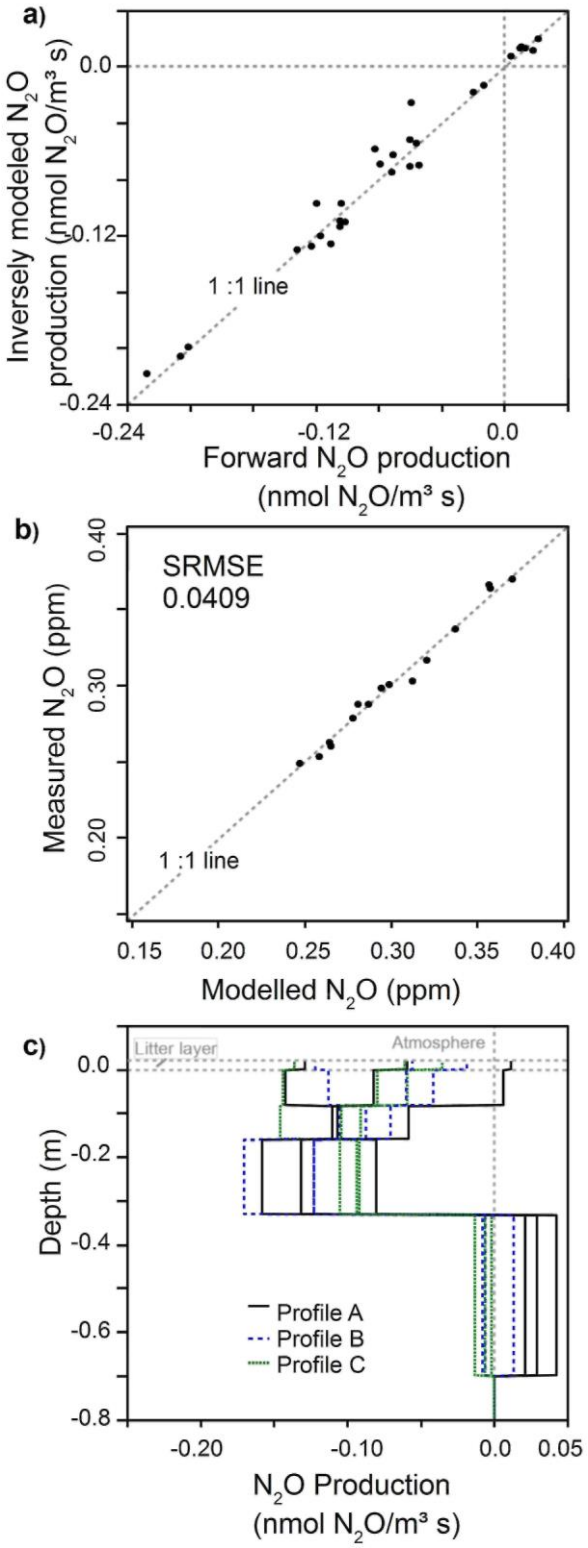

Published in : Agricultural and Forest Meteorology (2017), v. 247, pp. 21-33
DOI : 10.10i6/j.agrformet.2017.07.008
Status : Postprint (Author's version)

3.2.5 CONCENTRATIONS AND CONSUMPTION AND PRODUCTION OF N_2O IN THE SOIL PROFILE

Chamber measurements and the FEM approach showed that the soil was a sink for N_2O during our study. Soil-atmosphere fluxes ranged from -0.06 to -0.03 nmol m^{-2} s^{-1} (Table 3), agreeing with N_2O uptake observed at other sites (Butterbach-Bahl et al., 2002; Chapuis-Lardy et al., 2007; Rosenkranz et al., 2006). Soil N_2O concentrations were always below ambient concentrations and decreased with depth (Fig. 8a and b), reaching 0.16 ppm at 0.65m depth. N_2O concentrations fluctuated on a diurnal scale, but daily mean values showed stable temporal trends (online supplement). The N_2O concentrations in the subsoil were more scattered than in the topsoil. Below 0.3 m depth, the 2D N_2O profiles showed horizontal concentration gradients as high as the vertical gradients below 0.3 m depth (Fig. 8a and b).

Most of the N_2O consumption occurred in the topsoil reaching -0.23 nmol $m^{-3}s^{-1}$ (Fig 8c and d). Subsoil (> 0.35 m depth) N_2O fluxes were an order of magnitude smaller than the soil-atmosphere flux. Modeling yielded small negative and positive P^{N2O} values, and horizontal fluxes as large as vertical fluxes. The 2D profiles of P^{N2O} were more variable than CO_2 or CH_4. Soils can be sinks but also sources for atmospheric N_2O, depending on the prevailing process, consumption or production of N_2O (Chapuis-Lardy et al., 2007).

3.2.6 UNCERTAINTY IN THE MODELED N_2O CONSUMPTION AND PRODUCTION PROFILE

A sensitivity test using known ("forward") and inversely modeled 2D P^{N2O} profiles showed that the mean P^{N2O} values agreed reasonably (Table 1, Fig. 9a). Standard deviations were high, indicating that the horizontal variability was not properly reflected. Nevertheless, good agreement between measured and modeled N_2O concentrations (Fig 9b) was achieved by inverse modeling of the N_2O and P^{N2O} profiles, with SRMSE < 0.05 (Table 2). Including daily minimum and maximum soil N_2O concentrations in the inverse modeling resulted in wide minimum-maximum ranges of P^{N2O} (Fig. 9c), due to the scattering of the N_2O concentrations on the diurnal scale.

Chamber measurements and FEM derived soil-atmosphere fluxes were in the same order of magnitude, but mean values seemed to deviate. The observed difference in the mean N_2O flux, however, was not significant since the chamber measurements had a very high variability (Table 2). This variability probably results from N_2O consumption and production at the aggregate scale at hotspots (Chapuis-Lardy et al., 2007; Davidson and Verchot, 2000; Kuzyakov and Blagodatskaya, 2015) that can be expected in the microbial highly active moist litter layer. We have to consider that both N_2O production and N_2O consumption may occur simultaneously at different microsites next to each other (Conrad, 1996; Smith et al., 2003). The scale of the FEM model compartments was much larger than these microsites. Nevertheless, our 2D mapping approach can indicate the effective net process within the analyzed compartment.

The sensitivity tests showed that the inverse modeling step can introduce artifacts and have an important impact on the modeled 2D profiles. Using daily mean concentrations of N_2O reduced most of the scattering in the data. Knowing this, N_2O data have to be interpreted carefully.

3.3 MODELING ASPECTS

Simple sensitivity tests showed that the FEM approach could produce reasonable results for the 2D profiles of D_S/D_0, P^{CO2} and P^{CH4}.

Higher uncertainty has to be expected in the litter layer, and generally when P^{N2O} is modeled. This effect can be attributed to the small concentration gradients that were found in the litter layer for all gases, and especially in the N_2O soil profile where fluxes and gradients were minimal.

Published in : Agricultural and Forest Meteorology (2017), v. 247, pp. 21-33
DOI : 10.10i6/j.agrformet.2017.07.008
Status : Postprint (Author's version)

Additionally, the design of the physical model affects the results obtained, *e.g.* choosing several smaller or few larger soil compartments, or using discrete P^{CO2} values for the soil compartments or a mathematical function describing the whole P^{CO2} profile (Maier and Schack-Kirchner, 2014; Novak, 2007). Inverse modeling questions may be ill posed, and a penalty function required. Choosing the right penalty function is essential, since it favors certain structures in the optimized parameter. Both steps, the choice of the physical model and the penalty function affect the results of the modeling and have to be chosen carefully. However, leaving the physical model and the penalty function unchanged for all days modeled allowed us to reliably interpret the changes over the days.

3.4 FUTURE APPLICATIONS

Soil gas diffusivity needs to be known to interpret soil gas concentrations. Unfortunately, it is not possible to know *a priori* which of the existing diffusivity models fits a given soil best. Monitoring soil gas diffusivity over a longer time with changing soil water contents would allow deriving more realistic diffusivity models.

Our approach allowed analyzing spatial patterns of soil gas diffusivity and the production of GHG in the soil, and monitoring the temporal dynamics of these. Modeling soil gas transport in 3D should be a next step since most soils exhibit complex structures such as compacted zones, cracks, mouse holes or large roots. Combining the FEM approach with methods using isotopically labeled CO_2 (Hagedorn et al., 2016; Klein et al., 2016) would allow further investigation of the below ground allocation of carbon. Combining the FEM approach with methods that are able to map methanotrophic activity in the soil (Niklaus et al., 2016) would allow for a better understanding of methane consumption in soil.

4 Conclusions

We conclude that our new method represents a valuable tool for analyzing spatial and temporal variability of gas fluxes and production at a soil profile scale and that it will allow novel insights into the dynamics of soil gases. The method was able to produce reliable results if sufficiently strong gas concentration gradients occur. Further development must include the 3D investigation of soil gas processes in more complex soils.

ACKNOWLEDGEMENTS

We would like to thank Prof. Schmid, Center for Technomathematics, Bremen University, for their assistance with FEM, N. Koele for proofreading, and the German Research Foundation (DFG) for funding this research project (Ma- 5826/2-1). We also would like to thank the anonymous reviewer and M. Novak for their substantial contribution and constructive comments.

APPENDIX A. SUPPLEMENTARY DATA

Supplementary data associated with this article can be found, in the online version, at http://dx.doi.Org/10.1016/j.agrformet.2017.07.008.

Published in : Agricultural and Forest Meteorology (2017), v. 247, pp. 21-33
DOI : 10.10i6/j.agrformet.2017.07.008
Status : Postprint (Author's version)

References

Adamsen, A., King, G.M., 1993. Methane Consumption in Temperate and Subarctic Forest Soils: Rates, Vertical Zonation, and Responses to Water and Nitrogen. Appl. Environ. Microbiol. 59 (2), 485-490.

Allaire, S.E., Lafond, J.A., Cabral, A.R., Lange, S.F., 2008. Measurement of gas diffusionthrough soils: comparison of laboratory methods. J. Environ. Monit. 10 (11),1326-1336.

Ball, B., Smith, K.A., Klemedtsson, L., Brumme, R., Sitaula, B.K., Hansen, S., Priemé, A., MacDonald, J., Horgan, G.W., 1997. The influence of soil gas transport properties on methane oxidation in a selection of northern European soils. J. Geophys. Res. 102 (D19), 23309.

Borken, W., Beese, F., 2006. Methane and nitrous oxide fluxes of soils in pure and mixed stands of European beech and Norway spruce. Eur. J. Soil Sci. 57 (5), 617-625.

Butterbach-Bahl, K., Breuer, L., Gasche, R., Willibald, G., Papen, H., 2002. Exchange of trace gases between soils and the atmosphere in Scots pine forest ecosystems of the northeastern German lowlands. For. Ecol. Manage. 167 (1-3), 123-134.

Chapuis-Lardy, L., Wrage, N., Metay, A., Chotte, J.-L., Bernoux, M., 2007. Soils, a sink for N_2O? A review. Global Change Biol. 13 (1), 1-17.

Conrad, R., 1996. Soil microorganisms as controllers of atmospheric trace gases (H_2, CO, CH 4, OCS, N_2O and NO). Microbiol. Rev 60, 609-640. Davidson, E.A., Savage, K.E., Trumbore, S.E., Borken, W., 2006. Vertical partitioning of CO_2 production within a temperate forest soil. Global Change Biol. 12 (6), 944-956.

Davidson, E.A., Trumbore, S.E., 1995. Gas diffusivity and production of CO_2 in deep soils of the eastern Amazon. Tellus B 47 (5), 550-565.

Davidson, E.A., Verchot, L.V., 2000. Testing a Conceptual Model of Soil Emissions of Nitrous and Nitric Oxides. Global Biogeochem. Cycles 14 (4), 1035-1043.

DeJong, E., Schappert, H.J.V., 1972. Calculation of soil respiration and activity from CO_2 profiles in the soil. Soil Science 113 (5), 328-333.

FAO, 2006. World reference base for soil resources 2006: A framework for international classification, correlation and communication. FAO, Rome 128 pp.

Fischer, J.C., von Hedin, L.O., 2002. Separating methane production and consumption with a field-based isotope pool dilution technique. Global Biogeochem. Cycles 16 (3) 8-1-8-13.

Fuller, E.N., Schettler, P.D., Giddings, J.C., 1966. New method for prediction of binary gas/phase diffusion coefficients. Ind. Eng. Chem. 58 (5), 18-27.

Goffin, S., Aubinet, M., Maier, M., Plain, C, Schack-Kirchner, H., Longdoz, B., 2014. Characterization of the soil CO_2 production and its carbon isotope composition in forest soil layers using the flux-gradient approach. Agr. For. Met. 188, 45-57.

Goffin, S., Wylock, C, Haut, B., Maier, M., Longdoz, B., Aubinet, M., 2015. Modeling soil CO_2 production and transport to investigate the intra-day variability of surface efflux and soil CO_2 concentration measurements in a Scots Pine Forest (Pinus Sylvestris, L.). Plant Soil 390 (1-2), 195-211.

Published in : Agricultural and Forest Meteorology (2017), v. 247, pp. 21-33
DOI : 10.10i6/j.agrformet.2017.07.008
Status : Postprint (Author's version)

Hagedorn, F., Joseph, J., Peter, M., Luster, J., Pritsch, K., Geppert, U., Kerner, R., Molinier, V., Egli, S., Schaub, M., Liu, J.-F., Li, M., Sever, K., Weiler, M., Siegwolf, R.T.W., Gessler, A., Arend, M., 2016. Recovery of trees from drought depends on belowground sink control. Nature plants 2, 16111.

Hartmann, A.A., Buchmann, N., Niklaus, P.A., 2011. A study of soil methane sink regulation in two grasslands exposed to drought and N fertilization. Plant Soil 342 (1-2), 265-275.

Hoist, J., Barnard, R., Brandes, E., Buchmann, N., Gessler, A., Jaeger, L., 2008. Impacts of summer water limitation on the carbon balance of a Scots pine forest in the southern upper Rhine plain. Agr. For. Met. 148 (11), 1815-1826.

Jassal, R., Black, A., Novak, M., Morgenstern, K., Nesic, Z., Gaumont-Guay, D., 2005. Relationship between soil CO_2 concentrations and forest-floor CO_2 effluxes. Agr. For. Met. 130 (3-4), 176-192.

Jassal, R.S., Black, T.A., Drewitt, G.B., Novak, M.D., Gaumont-Guay, D., Nesic, Z., 2004. A model of the production and transport of CO_2 in soil: Predicting soil CO_2 concentrations and CO_2 efflux from a forest floor. Agr. For. Met. 124 (3-4), 219-236.

Karbin, S., Hagedorn, F., Hiltbrunner, D., Zimmermann, S., Niklaus, P.A., 2016. Spatial micro-distribution of methanotrophic activity along a 120-year afforestation chronosequence. Plant Soil 31, 978.

Klein, T., Siegwolf, R.T.W., Korner, C, 2016. Belowground carbon trade among tall trees in a temperate forest. Science 352 (6283), 342-344.

Kuhne, A., Schack-Kirchner, H., Hildebrand, E.E., 2012. Gas diffusivity in soils compared to ideal isotropic porous media. J. Plant Nutr. Soil Sci. 175 (1), 34-45.

Kuzyakov, Y., Blagodatskaya, E., 2015. Microbial hotspots and hot moments in soil: Concept & review. Soil Biol. Biochem. 83, 184-199.

Laemmel, T., Maier, M., Schack-Kirchner, H., Lang, F., 2017. An in situ method for realtime measurement of gas transport in soil. Eur. J. Soil Sci. 68 (2), 156-166.

Lange, S.F., Allaire, S.E., Rolston, D.E., 2009. Soil-gas diffusivity in large soil monoliths. Eur. J. Soil Sci. 60 (6), 1065-1077.

Levy, P.E., Gray, A., Leeson, S.R., Gaiawyn, J., Kelly, M.P.C., Cooper, M.D.A., Dinsmore, K.J., Jones, S.K., Sheppard, L.J., 2011. Quantification of uncertainty in trace gas fluxes measured by the static chamber method. Eur. J. Soil Sci. 62 (6), 811-821.

Maier, M., Machacova, K., Lang, F., Svobodova, K., Urban, O., 2017. Combining soil and tree-stem flux measurements and soil gas profiles to understand CH_4 pathways in *Fagus sylvatica* forests. J. Plant Nutr. Soil Sci. 21, 53.

Maier, M., Schack-Kirchner, H., 2014. Using the gradient method to determine soil gas flux: A review. Agr. For. Met. 192-193, 78-95.

Maier, M., Schack-Kirchner, H., Aubinet, M., Goffin, S., Longdoz, B., Parent, F., 2012. Turbulence Effect on Gas Transport in Three Contrasting Forest Soils. Soil Sci. Soc. Am. J. 76 (5), 1518.

Maier, M., Schack-Kirchner, H., Hildebrand, E.E., Hoist, J., 2010. Pore-space CO_2 dynamics in a deep, well-aerated soil. Eur. J. Soil Sci. 61 (6), 877-887.

Marrero, T.R., Mason, E.A., 1972. Gaseous Diffusion Coefficients. J. Phys. Chem. Ref. Data 1 (1), 3.

Massman, W.J., 1998. A review of the molecular diffusivities of H_2O, CO_2, CH_4, CO,O_3, SO_2, NH_3, N_2O, NO, and NO_2 in air, O_2 and N2 near STP. Atmos. Environ. 32 (6), 1111-1127.

Millington, R.J., Quirk, J.P., 1961. Permeability of porous solids. Trans. Faraday Soc. 57,1200.

Published in : Agricultural and Forest Meteorology (2017), v. 247, pp. 21-33
DOI : 10.10i6/j.agrformet.2017.07.008
Status : Postprint (Author's version)

Moldrup, P., Olesen, T., Gamst, J., Schjønning, P., Yamaguchi, T., Rolston, D.E., 2000. Predicting the Gas Diffusion Coefficient in Repacked Soil. Soil Sci. Soc. Am. J. 64 (5), 1588.

Moldrup, P., Olesen, T., Rolston, D.E., Yamaguchi, T., 1997. Modeling diffusion and reaction in soils: VII. Predicting gas and ion diffusivity in undisturbed and sieved soils. Soil Sci. 162 (9), 632-640.

Myklebust, M.C., Hipps, L.E., Ryel, R.J., 2008. Comparison of eddy covariance, chamber, and gradient methods of measuring soil $C0_2$ efflux in an annual semi-arid grass, *Bromus tectorum.* Agr. For. Met. 148 (11), 1894-1907.

Niklaus, P.A., Le Roux, X., Poly, F., Buchmann, N., Scherer-Lorenzen, M., Weigelt, A., Barnard, R.L., 2016. Plant species diversity affects soil-atmosphere fluxes of methane and nitrous oxide. Oecologia 181 (3), 919-930.

Novak, M.D., 2007. Determination of soil carbon dioxide source-density profiles by inversion from soil-profile gas concentrations and surface flux density for diffusion-dominated transport. Agr. For. Met. 146 (3-4), 189-204.

Parent, F., Plain, C, Epron, D., Maier, M., Longdoz, B., 2013. A new method for continuously measuring the δ^{13} C of soil CO_2 concentrations at different depths by laser spectrometry. Eur. J. Soil Sci. 64 (4), 516-525.

Pingintha, N., Leclerc, M.Y., Beasley Jr., J.P., Zhang, G., Senthong, 2010. Assessment of the soil CO_2 gradient method for soil CO_2 efflux measurements: Comparison of six models in the calculation of the relative gas diffusion coefficient. Tellus B 62 (1), 47-58.

Raw, C, Raw, T.T., 1976. Diffusion of gaseous fluoromethanes in air. Chem. Phys. Lett. 44 (2), 255-256.

Rosenkranz, P., Bruggemann, N., Papen, H., Xu, Z., Seufert, G., Butterbach-Bahl, K., 2006. N_2O, NO and CH_4 exchange, and microbial N turnover over a Mediterranean pine forest soil. Biogeosciences 3 (2), 121-133.

Sánchez-Cañete, E.P., Kowalski, A.S., 2014. Comment on Using the gradient method to determine soil gas flux: A review by M. Maier and H. Schack-Kirchner. Agr. For. Met. 197, 254-255.

Smith, K.A., Ball, T., Conen, F., Dobbie, K.E., Massheder, J., Rey, A., 2003. Exchange of greenhouse gases between soil and atmosphere: Interactions of soil physical factors and biological processes. Eur. J. Soil Sci. 54 (4), 779-791.

The physical science basis: Contribution of Working Group I to the Fourth Assessment Report of the Intergovernmental Panel on Climate Change. In: Solomon, S. (Ed.), 1. publ ed. VIII, 996 S.

Stiehl-Braun, P.A., Hartmann, A.A., Kandeler, E., Buchmann, N., Niklaus, P.A., 2011. Interactive effects of drought and N fertilization on the spatial distribution of methane assimilation in grassland soils. Global Change Biol. 17 (8), 2629-2639.

Tang, J., Baldocchi, D.D., Qi, Y., Xu, L., 2003. Assessing soil CO_2 efflux using continuous measurements of CO_2 profiles in soils with small solid-state sensors. Agr. For. Met. 118 (3-4), 207-220.

Tang, J., Baldocchi, D.D., Xu, L., 2005. Tree photosynthesis modulates soil respiration on a diurnal time scale. Global Change Biol. 11 (8), 1298-1304.

van Bochove, E., Bertrand, N., Caron, J., 1998. *In situ* estimation of the gaseous nitrous oxide diffusion coefficient in a sandy loam soil. Soil Sci. Soc. Am. J. 62 (5), 1178.

Vargas, R., Allen, M.F., 2008. Dynamics of Fine Root, Fungal Rhizomorphs, and Soil Respiration in a Mixed Temperate Forest: Integrating Sensors and Observations. Vadose Zone J. 7 (3), 1055.

Published in : Agricultural and Forest Meteorology (2017), v. 247, pp. 21-33
DOI : 10.10i6/j.agrformet.2017.07.008
Status : Postprint (Author's version)

von Fischer, J.C., Butters, G., Duchateau, P.C., Thelwell, R.J., Siller, R., 2009. In situ measures of methanotroph activity in upland soils: A reaction-diffusion model and field observation of water stress. J. Geophys. Res. 114 (Gl).

Werner, D., Grathwohl, P., Hohener, P., 2004. Review of Field Methods for the Determination of the Tortuosity and Effective Gas-Phase Diffusivity in the Vadose Zone. Vadose Zone J. 3 (4), 1240-1248.

Wilhelm, E., Battino, R., Wilcock, R.J., 1977. Low-pressure solubility of gases in liquid water. Chem. Rev. 77 (2), 219-262.